



---

**Forschungszentrum Karlsruhe**  
in der Helmholtz-Gemeinschaft

---

**Wissenschaftliche Berichte**  
FZKA 7196

**Actinide Migration Experiment  
in the ÄSPÖ HRL in Sweden:  
Analysis of Retained Uranium  
and Technetium in Core #7  
(Part V)**

**B. Kienzler, P. Vejmelka, J. Römer,  
B. Luckscheiter, T. Kisely, E. Soballa,  
C. Walschburger, A. Seither**

**Institut für Nukleare Entsorgung**

**Februar 2006**



**Forschungszentrum Karlsruhe**

in der Helmholtz-Gemeinschaft

Wissenschaftliche Berichte

FZKA 7196

Actinide Migration Experiment in the  
ÄSPÖ HRL in Sweden: Analysis of Retained  
Uranium and Technetium in Core #7 (Part V)

B. Kienzler, P. Vejmelka, J. Römer, B. Luckscheiter,  
T. Kisely, E. Soballa, C. Walschburger, A. Seither

Institut für Nukleare Entsorgung

Forschungszentrum Karlsruhe GmbH, Karlsruhe

2006

Für diesen Bericht behalten wir uns alle Rechte vor

Forschungszentrum Karlsruhe GmbH  
Postfach 3640, 76021 Karlsruhe

Mitglied der Hermann von Helmholtz-Gemeinschaft  
Deutscher Forschungszentren (HGF)

ISSN 0947-8620

urn:nbn:de:0005-071968

**Actiniden-Migrationsexperiment im schwedischen Untertagelabor ÄSPÖ:  
Analyse des sorbierten Urans und Technetiums in Core #7 (Teil V)**

Im Rahmen einer bilateralen Kooperation wurde eine Reihe von **Actiniden-Migrationsexperimenten** vom INE im schwedischen Untertagelabor Äspö durchgeführt. Neben mehreren Experimenten zur Migration der Actiniden Am, Np und Pu, wurden die Untersuchungen zur Uran- und Technetium-Migration in einer Kluft im Granit (core #7) bereits vorgestellt und die Durchbruchskurven sowie der Wiedererhalt dieser Elemente diskutiert. Der Wiedererhalt des  $^{233}\text{U}$  Tracers betrug ca. 40 %, von  $^{99}\text{Tc}$  etwa 1 %. Mit dem  $R_s$ -Wert, der für Uran sowohl aus Batch als auch aus dem in-situ Versuch abgeleitet wurde, ist der gemessene Wiedererhalt bezogen auf die lange Versuchszeit und eluiertes Volumen gering. Aus diesem Grund ist die Analyse der Verteilungen beider Elemente im Bohrkern #7 längs des Migrationspfades von großem Interesse. Es werden die Ergebnisse der verschiedenen Analysemethoden vorgestellt und die Befunde diskutiert.

Auf Grund des Durchbruchverhaltens des  $^{233}\text{U}$  Tracers sowie des natürlichen Urans aus dem Bohrkern, wurde vor Beendigung des Migrationsexperiments eine Unterbrechung des Durchflusses vorgenommen, um weitere Informationen zur Mobilisierung von natürlichem Uran aus dem Gestein des Bohrkerns zu erhalten. Diese Befunde werden ebenfalls dargestellt und diskutiert.

## Abstract

Within the scope of a bilateral cooperation a series of **Actinide Migration Experiment** were performed by INE at the Äspö Hard Rock Laboratory in Sweden. Besides several experiments investigating the migration of the actinides Am, Np and Pu, investigations on uranium and technetium migration in a single fractured granite sample (core #7) have been presented in a previous report which covers breakthrough and recovery of these tracers. In the case of  $^{233}\text{U}$ , recovery was determined in the range of 40 %, for Tc about 1%. Application of  $R_s$  determined by batch and in-situ experiments for uranium shows that observed recovery is relatively small. For this reason, analyses of the distribution of retained tracers in core #7 are significant. The results obtained by different methods are presented and discussed.

The  $^{233}\text{U}$  tracer and the natural uranium showed distinguished elution behaviour. To obtain deeper insight into the mobilization the natural uranium, the migration experiment was interrupted for a certain period before termination of the experiment. These results are also presented and discussed.

## TABLE OF CONTENTS

1	Background and Objectives .....	1
2	Properties of the fractured drill core # 7 .....	2
3	U in-situ migration experiment.....	3
3.1	Cocktail.....	3
3.2	Performance of the in-situ migration experiment.....	3
3.3	Analysis of abraded solid.....	4
3.4	Composition of the solids.....	5
3.5	Visual appearance and sorbed radionuclides.....	7
4	Interpretation and discussion of results.....	7
4.1	Breakthrough and mobilisation of uranium .....	7
4.2	Mineralogical characterization of the fracture zone .....	8
4.3	Uranium retention .....	12
4.4	Technetium retention .....	14
5	Conclusions.....	14
6	References.....	16
Appendix A	Images of slices of core #7 .....	17

## FIGURES

Fig. 1	3 D (voxel) representation of the fracture in core #7 determined from X-ray tomography data.	2
Fig. 2	Breakthrough of natural $^{238}\text{U}$ and $^{233}\text{U}$ tracers during the duration of the migration experiment with core #7.	4
Fig. 3	Concentrations of $^{99}\text{Tc}$ and $^{233}\text{U}$ tracers and natural U in the abraded material of core #7.	5
Fig. 5	Distribution of main elements in abraded material of core #7.	6
Fig. 6	Distribution of trace elements in abraded material of core #7.	6
Fig. 4	Comparison between different slices of core #7.	7
Fig. 7	XRD patterns of the abraded material at positions A, B, C and D.	9
Fig. 8	Details of the XRD patterns at positions A (black) and C (red).	9
Fig. 9	SEM (left) and optical (right) image of the flow path in the fracture at slice #23 (position C, X = 100 mm).	10
Fig. 10	Ca and Fe distribution along the SEM/EDX line scan in slice 23 (X = 100 mm).	11
Fig. 11	Main element distributions along the line shown in Fig. 5 and 6 from top to bottom.	11
Fig. 12	Lateral element mapping of the fracture zone of slice 23 from core #7.	12





# 1 Background and Objectives

The Äspö Hard Rock Laboratory (HRL) was established in Sweden in a granite rock formation for in-situ testing of radioactive waste disposal techniques and for investigations concerning migration and retention of radionuclides (Bäckblom, 1991). Groundwater flow through fractures in granite host rocks may cause migration of radionuclides from the repository. Within the scope of a bilateral cooperation between Svensk Kärnbränslehantering AB (SKB) and Forschungszentrum Karlsruhe, Institut für Nukleare Entsorgung (FZK-INE), actinide migration experiments with Pu, Am, and Np have been conducted in laboratory and under in-situ conditions at the Äspö Hard Rock Laboratory since the year 1999 (Kienzler et al., 2002; Kienzler et al., 2003b; Kienzler et al., 2003c; Kienzler et al., 2005; Römer et al., 2002; Vejmelka et al., 2000). The present report is the second concerning the in-situ experiments with uranium and technetium in core #7. It covers the pending results concerning the distribution of retained tracers in core #7 as well as natural uranium and tracer breakthrough after interruption of the in-situ migration experiment with core #7 for a certain period.

The objectives of the FZK-INE investigations are focusing on the quantification of the retention of different actinide elements in individual fractures of a granite host rock and the investigation of the sorption mechanisms. Furthermore, the in-situ actinide migration experiments in the Äspö HRL are directed to examine the applicability of laboratory data to natural conditions and to verify the laboratory sorption studies. Investigations have been performed previously with the actinides Am, Np and Pu. Retention experiments of U and Tc have been done with granite and "fracture filling material" in laboratory. Results are presented elsewhere (Kienzler et al., 2003a; Kienzler et al., 2003c; Kienzler et al., 2005). Migration experiments with HTO, U and Tc through an individual fracture in a drill core have been performed in the Äspö HRL since May 2004 (Kienzler et al., 2005). To establish realistic conditions - as close to nature as possible - the experiments are performed in the CHEMLAB 2 probe (Jansson and Eriksen, 1998). This probe confines the drill core, the reservoir with the tracers and the required pump, valves, tubing and control systems. The drill hole interferes a groundwater-bearing fracture at a distance of several meters from the HRL tunnel (Chemlab 2 drill hole KJ0044F01). Details on the solid materials and the groundwater used in the experiments can be found in a previous publication (Kienzler et al., 2003c).

Investigations of the flow path properties and the breakthrough of inert HTO tracer are reported (Kienzler et al., 2005). Breakthrough of the  $^{233}\text{U}$  tracer shows a complex pattern. Initially, a slightly retarded peak in comparison to HTO appears which is followed by a broad U distribution. After an interruption of the experiment, a sharp  $^{233}\text{U}$  peak is observed. The migration velocity of the broad  $^{233}\text{U}$  distribution agrees well with the predicted U(VI) migration based on retardation coefficients obtained from batch experiments. Natural  $^{238}\text{U}$  which was not present in the used tracer shows a similar pattern as the  $^{233}\text{U}$  tracer. The concentrations of natural U are interpreted by oxidation of natural uranium in the core. Breakthrough of  $^{99}\text{Tc}$  is observed simultaneously with HTO. Observed Tc recovery is in the range of about 1%.

## 2 Properties of the fractured drill core # 7

Mechanical properties of core #7, X-ray tomography, fracture geometry and aperture, confinement into a steel autoclave and hydraulic properties are reported previously (Kienzler et al., 2003c; Kienzler et al., 2005). The aperture for the fracture in the core #7 was determined to be in the range of 0.8 mm. For core #7, the maximum areas of the open fracture (100 mm<sup>2</sup>) are located at a distance of 30 mm, and between 80 mm and 110 mm from the injection. Minima areas of the open fracture occur in the range from the input to 30 mm (below 40 mm<sup>2</sup>).

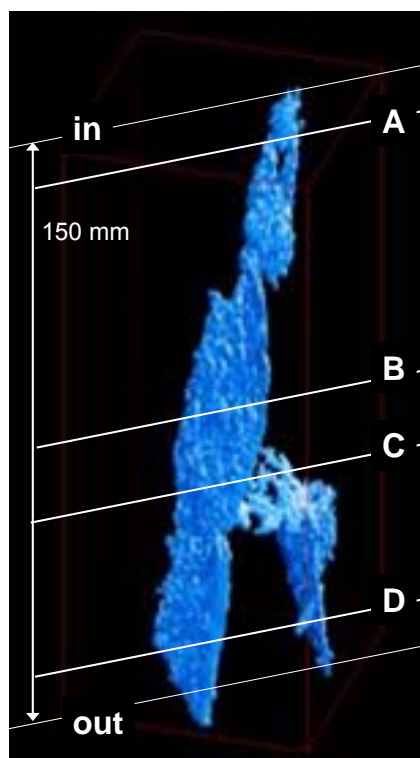


Fig. 1 3 D (voxel) representation of the fracture in core #7 determined from X-ray tomography data.

Lines A, B, C and D are referred to in the following chapters

Fig. 1 shows the complex structure of the fracture. At the bottom of the 3D representation (indicated by “out”), two fractures are present having certain connectivity. At the top of the picture (indicated by “in”), the single fracture is twisted. The hydraulic data are evaluated as described in (Vejmelka et al., 2001). The effective porosity of the core was determined between 1.9 and 2.3 ml.

## 3 U in-situ migration experiment

### 3.1 Cocktail

For the in-situ migration experiment with core #7, a cocktail was applied consisting of groundwater SA 2600 spiked by  $1.35 \times 10^{-6} \text{ mol l}^{-1} \text{ }^{233}\text{U}$ ,  $7.0 \times 10^{-7} \text{ mol l}^{-1} \text{ }^{99}\text{Tc}$  and  $370 \text{ Bq ml}^{-1}$  HTO. pH of the cocktail was 7.3, Eh about +70 mV. The concentration of the natural uranium isotope  $^{238}\text{U}$  was  $2.3 \times 10^{-9} \text{ mol l}^{-1}$ , significantly below the  $^{233}\text{U}$  tracer concentration.

### 3.2 Performance of the in-situ migration experiment

The core #7 and the cocktail were transferred to Äspö HRL, inserted into Chemlab 2 and a pre-equilibration phase was started in March 2004. After 6 weeks, the flow rate was adjusted to 0.03 to 0.05 ml h<sup>-1</sup>. In total 10.6 ml of cocktail were injected within a period of 342 hours (14.3 days). Sampling of eluted groundwater was performed by an automatic sampler, changing vials after each 30 hours interval. The vials were sealed to avoid evaporation. Within the first few days, an operating error of the sampler occurred and several sampled volumes have to be united for analysis. The first phase of the experiment lasted from May 13 to July 30, 2004, delivering 62 samples. After the restart of Chemlab 2 in September 3, additional 110 groundwater samples were collected until January 19, 2005. The migration experiment was continued until February 28. In order to obtain additional insight into the mobilization the natural uranium, the migration experiment was interrupted for a period of 3 weeks (until March 21, 2005). Then the experiment was started again and samples were collected until April 14. At this date the experiment was terminated. All samples were analysed at Forschungszentrum Karlsruhe. Fig. 2 shows the eluted concentrations of the  $^{233}\text{U}$  tracer and the natural  $^{238}\text{U}$  as function of the duration of the experiment.

Except for the vacation period during August 2004 and some one-day stops due to works on the electricity supply of Äspö HRL, Chemlab 2 worked without any problem. Correct operation of Chemlab 2 was shown in the previous report. The experiment was interrupted from July 30 to September 03, 2004, for another 2 days in October and finally the intentional interruption of 3 weeks in March 2005. The scatter of  $^{233}\text{U}$  concentrations between beginning and end of June 2004 is the result of using both LSC and ICP-MS measurements in the same diagram.

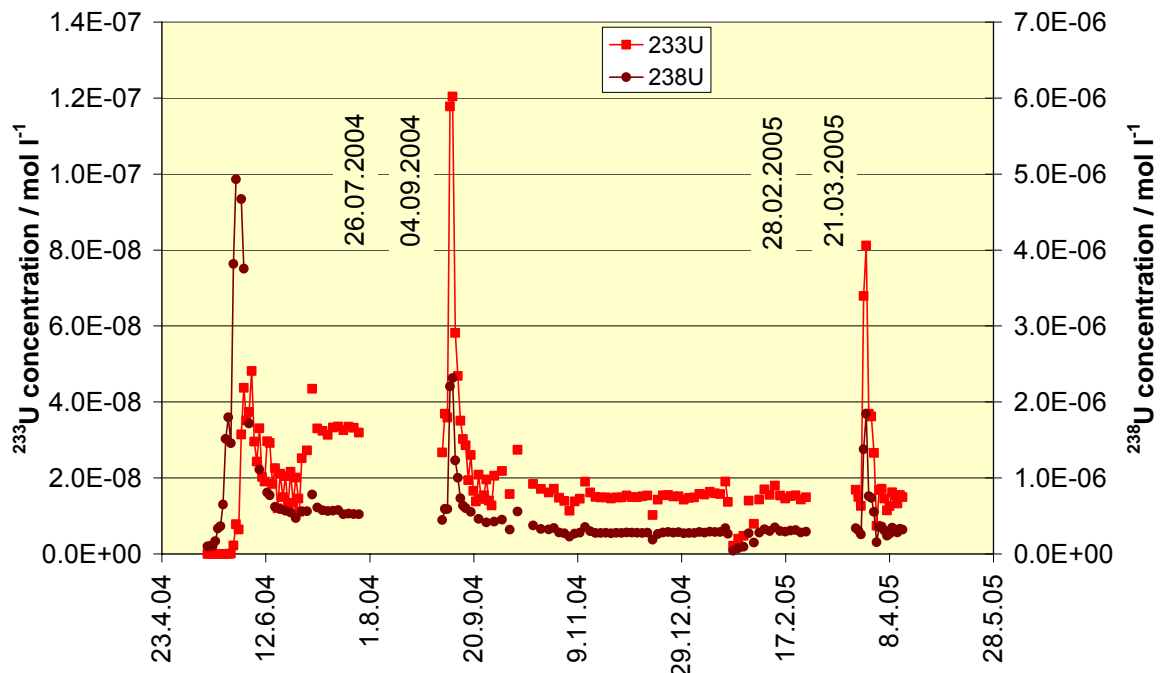


Fig. 2 Breakthrough of natural  $^{238}\text{U}$  and  $^{233}\text{U}$  tracers during the duration of the migration experiment with core #7.

The  $^{233}\text{U}$  tracer and natural  $^{238}\text{U}$  show an initial peak close to the HTO peak. After the interruptions of the experiment in August 2004 and in March 2005, pronounced peaks for the U tracer and the natural U occur. The errors bars indicated in both figures are obtained by error propagation assuming a 10% error in each volume determination and 5% error in the ICP-MS concentration measurements.

The shoulder of the  $^{233}\text{U}$  concentration between middle of June and the interruption is attributed to sorption processes with a retardation coefficient of  $\sim 5$  (Kienzler et al., 2005).

### 3.3 Analysis of abraded solid

After termination of the experiment, core #7 was transferred to FZK-INE, cut in slices and analysed with respect to the sorbed tracers and matrix elements. Different from previous experiments, it was not possible to fill the open fracture with fluorescence resin. The abraded material from cutting was sampled, dissolved and analysed by ICP-MS. Fig. 3 shows the  $^{99}\text{Tc}$  and  $^{233}\text{U}$  distributions along core #7 as well as the distribution of natural uranium. In a distance of  $\sim 100$  mm (position C in Fig. 1) from injection, significant concentrations of natural U and  $^{233}\text{U}$  tracer are found. Also the  $^{99}\text{Tc}$  concentration is increased in this region. In contrast to uranium, a decrease of the thorium concentration (from  $\sim 8$  ppm to  $\sim 4$  ppm) is found in this region.

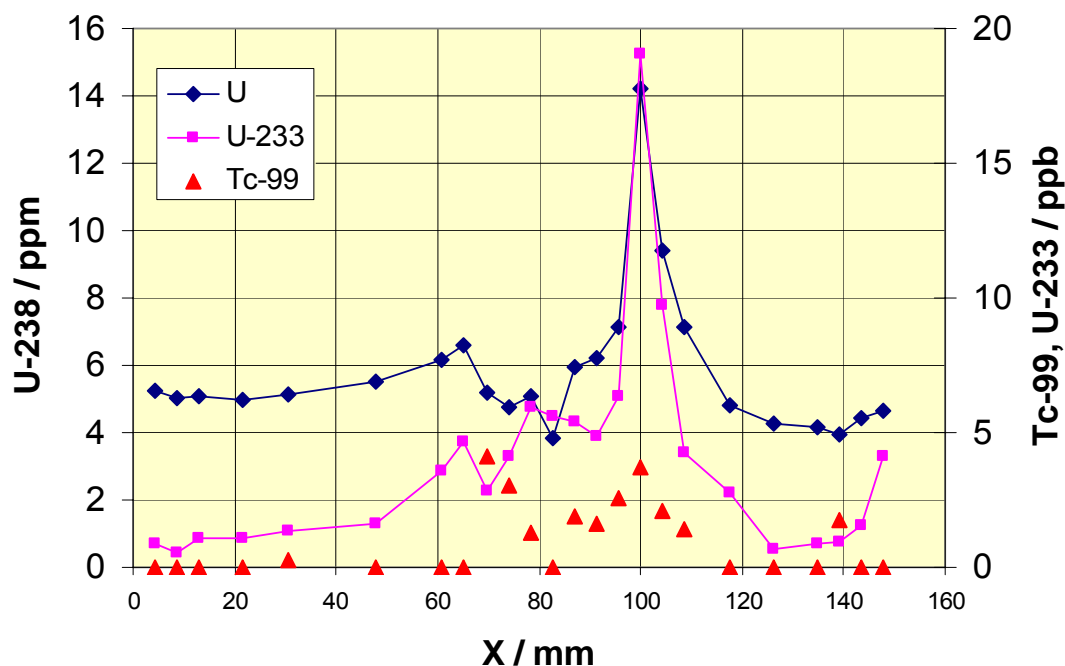


Fig. 3 Concentrations of  $^{99}\text{Tc}$  and  $^{233}\text{U}$  tracers and natural U in the abraded material of core #7.

The accuracy of element concentrations in the abraded material was tested by comparison with certified reference granite<sup>a</sup>. Errors of measured element concentrations result from errors of the weighted samples during the dissolution process and inaccurateness in the ICP-MS measurements. The accurateness of the whole process was tested by application of the process to standard granite. Deviations occur for the matrix elements such as Fe. For this reason, iron was measured by ICP-AES technique. Total errors of reported concentrations are in the range of 5 to 10 %.

### 3.4 Composition of the solids

Fig. 4 shows the distribution of main elements in the abraded material in the slices of core #7. Positions defined in Fig. 6 are marked in this figure. In the region of high uranium concentration (C), matrix elements show also deviations from the average values in the core: Mg concentration is decreased by a factor  $\sim 5$ , Ca is increased by about 2. Al shows also a higher concentration in comparison to the rest of core #7. Fe and K show also deviations from average values. These data cover average values, representing the complete diameter of the  $\varnothing 52$  mm drill core.

<sup>a</sup> LGC Promochem Rock – Constituents NCS DC73301

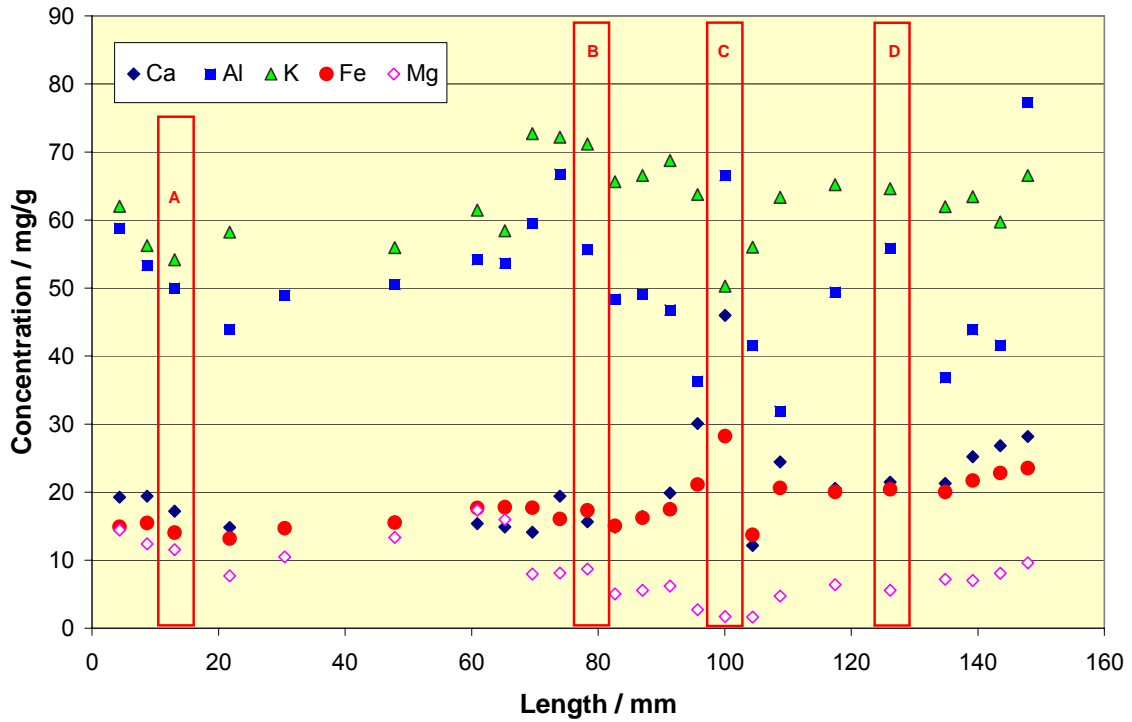


Fig. 4 Distribution of main elements in abraded material of core #7.

Distribution of trace elements in the abraded material of core #7 are shown in Fig. 5. A significantly lower concentration of Zr at location C is found (about 37 % of the mean value from all slices). At position C also an increase of 30% of La, 20 % of Ce and 60 % of Pb in comparison to the mean value is found. Nd concentration corresponds to the mean value.

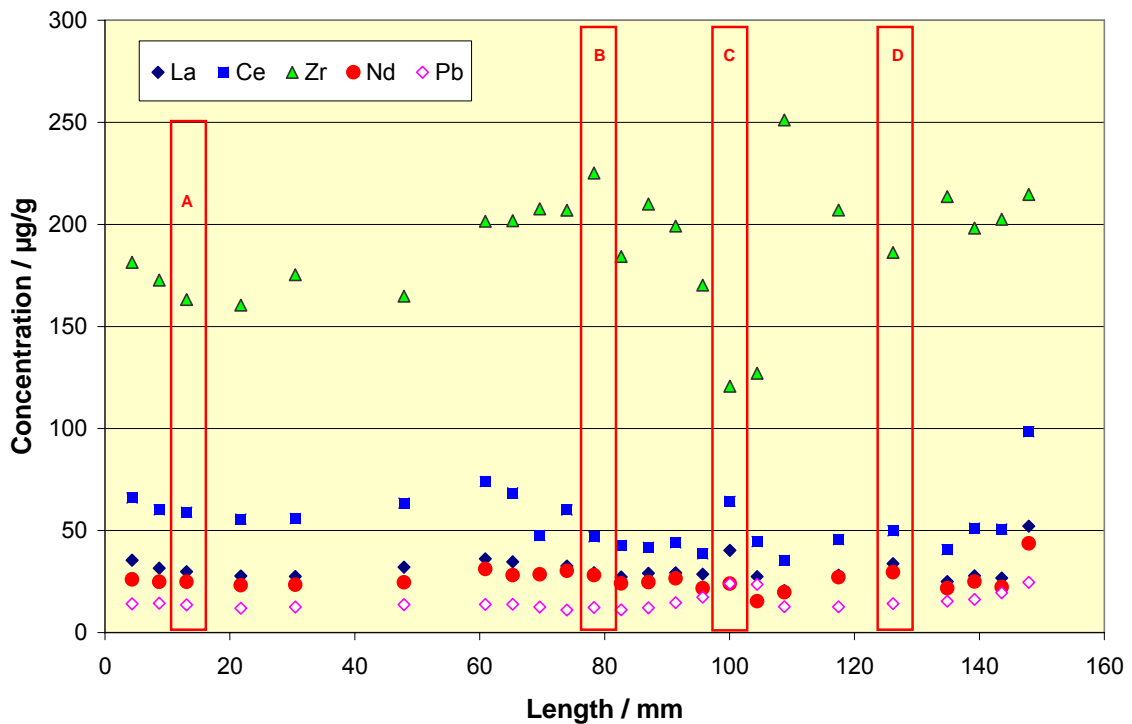
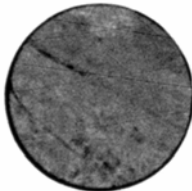
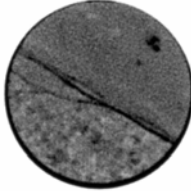
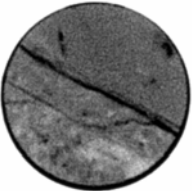
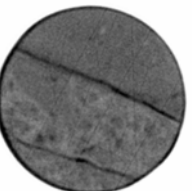
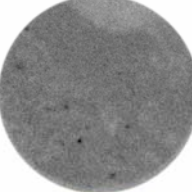
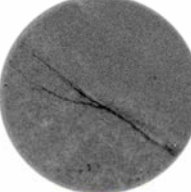
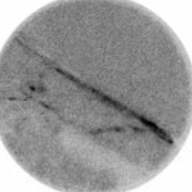
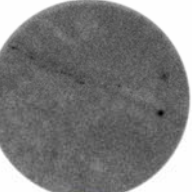

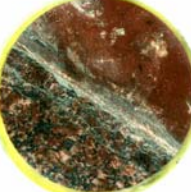
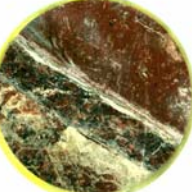
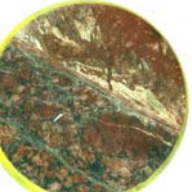


Fig. 5 Distribution of trace elements in abraded material of core #7.

### 3.5 Visual appearance and sorbed radionuclides

The slices obtained from core #7 are analyzed by different methods. The radioactivity of the slices was measured by an  $\alpha$ -autoradiography instrument using  $\alpha$ - and  $\beta$ -sensitive sheets. As described in ref.(Kienzler et al., 2003c), the  $\alpha$ -autoradiography and the optical information of the slices were combined. A comparison for some slices is shown in Fig. 6. The comparison reveals the fracture as expected from Fig. 1. At position C (~100 mm) a splitting of the single fracture in two fractures occurs.  $\alpha$ -autoradiography shows penetration of  $^{233}\text{U}$  in the second fracture. In the optical image, different colours indicate changes of the mineralogical compositions. At a depth of 130 mm (D), no sorbed  $^{233}\text{U}$  tracer is detected at the surfaces of the second fracture. This finding indicates that for radionuclide transport the main fracture (see Fig. 1) is dominating for groundwater transport.

Fig. 6 Comparison between different slices of core #7.

X / mm	13 ( A )	80 ( B )	100 ( C )	130 ( D )
X-ray tomography				
$\alpha$ -autoradiography				
Visual appearance				

## 4 Interpretation and discussion of results

### 4.1 Breakthrough and mobilisation of uranium

The simultaneous breakthrough of the artificial and of the natural uranium raises questions: In granite, U(IV) is expected which is kept in the tetravalent state by the presence of Fe(II) minerals. The U concentration in equilibrium with U(IV) minerals, such as  $\text{UO}_2(\text{am})$  would result for the in concentrations of  $1 \times 10^{-9} \text{ mol l}^{-1}$  which is in good agreement with the measured data. However, in core #7 experiments, after more than 200 days elapsed time, the eluted  $^{238}\text{U}$  concentration was in the range  $2\text{-}3 \times 10^{-7} \text{ mol l}^{-1}$  which surmounts the  $^{233}\text{U}$  con-

centration by a factor of ~20. Several assumptions are considered to explain the natural U concentrations: The assumptions cover a pH drop, increase of CO<sub>2</sub> partial pressure, and effects due to oxygen contamination either in the Chemlab 2 drill hole KJ0044F01, in the Chemlab 2 probe or in core #7. pH increase is ruled out and is additionally confirmed by the constant concentrations of mineral forming elements. Increase of CO<sub>2</sub> would also affect the pH.

The interpretation of the uranium breakthrough bases on the hypothesis that both uranium isotopes are present in the hexavalent redox state in solution and the solubility is controlled by hexavalent mineral phases. The prominent source of oxygen is air which contacted the rock matrix of core since drilling and during storage. Another source is oxygen migration through the excavated disturbed zone in the groundwater bearing fracture. To obtain information, redox measurements at the Chemlab 2 drill hole were performed (flow through cell) yielding a mean redox potential  $E_h = +248$  mV (SHE). To obtain insight in the U mobilisation and transport behaviour of uranium, the core # 7 experiment was interrupted for three weeks (from February 28, 2005). Fig. 1 shows the pronounced concentration peaks of both the artificial <sup>233</sup>U tracer and the natural <sup>238</sup>U. Both peaks decreased after elution of ~ 6 ml. This behaviour cannot be described by a pre-oxidation of U in the water bearing feature; the U oxidation/mobilisation process takes place within the core.

## 4.2 Mineralogical characterization of the fracture zone

At position C (X = 100 mm), a significant increase of measured <sup>233</sup>U tracer and natural <sup>238</sup>U is observed. The reason for this accumulation may be attributed to the quantity and composition of altered fracture materials or of the geometric instance of the fracture. As shown above, in this region of core #7 the fracture geometry changes. Mg and Ca concentrations change also indicating the dominance of different minerals in the abraded material at this part of the fracture. For this reason, detailed analyses of the mineralogical compositions are investigated by XRD and scanning electron microscope (SEM/EDX). XRD is performed with the abraded material at the positions A, C and D (see fig. 1). Positions A and D represent core #7, position C is situated at the maximum U concentration.

Fig. 7 shows identified minerals at the different positions: Clearly identified are diopside (CaMgSi<sub>2</sub>O<sub>6</sub>), orthoclase (KAlSi<sub>3</sub>O<sub>8</sub>), clinopyroxene ((Mg<sub>0.6</sub>Fe<sub>0.2</sub>Al<sub>0.2</sub>)Ca(Si<sub>1.5</sub>Al<sub>0.5</sub>)O<sub>6</sub>), and a potassium calcium aluminium silicate hydrate (zeolite). In the material close to the maximum U concentration at position C, traces of vaterite (CaCO<sub>3</sub>) may be present. Significant differences in the XRD patterns are only found for position C in comparison to the other parts of the core (see Fig. 8).



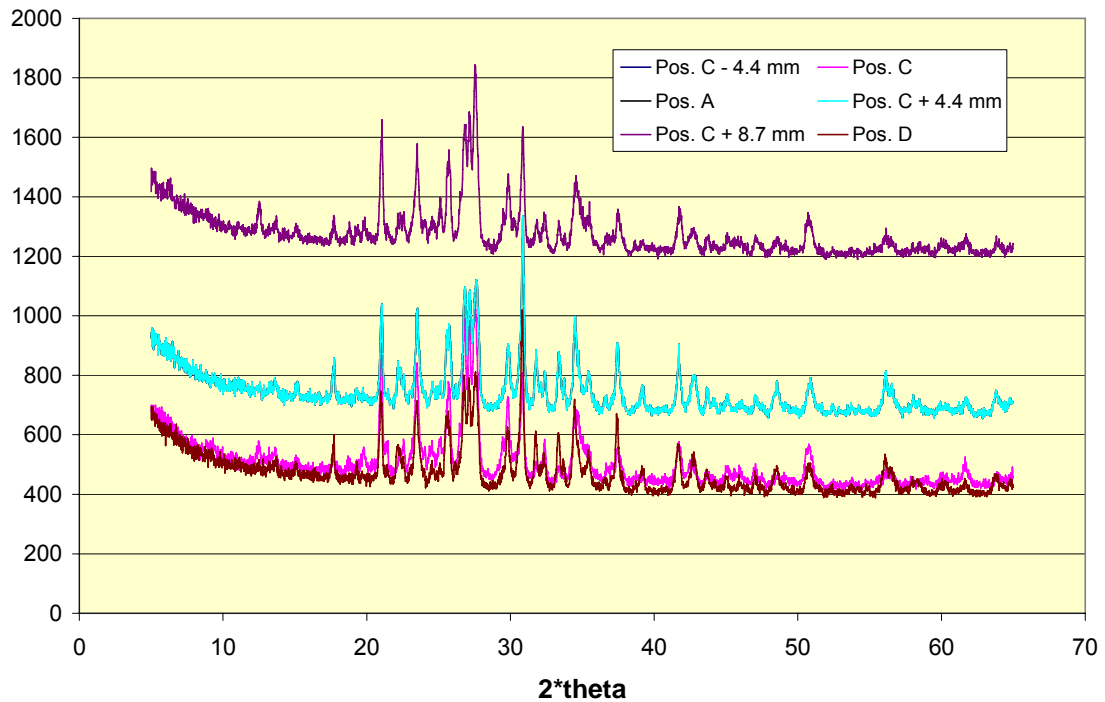


Fig. 7 XRD patterns of the abraded material at positions A, B, C and D.

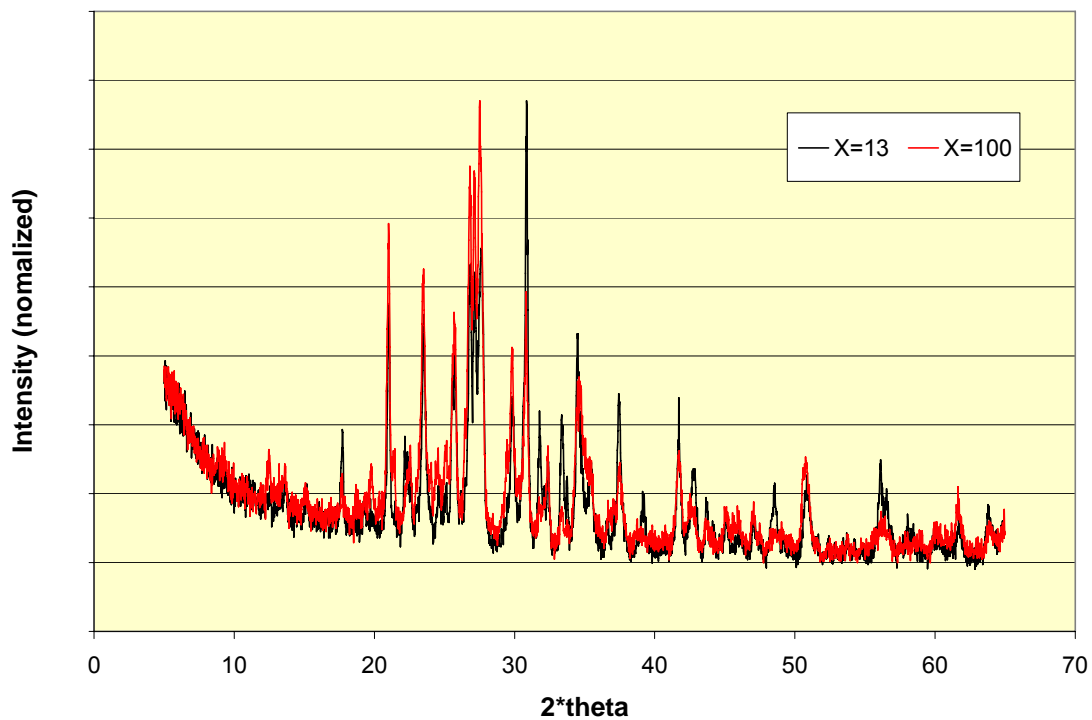


Fig. 8 Details of the XRD patterns at positions A (black) and C (red).

By means of REM techniques the slice (#23) of the highest U concentration is investigated. Fig. 9 reveals the electron microscopic and the optical picture of a location of the fracture with the highest radioactivity concentration. This was previously determined by  $\alpha$ -radiography. The U concentration in the solids is too low for detection by XRD or SEM/EDX.

The SEM image shows a part of the open fracture and the split up of the fracture. The visual appearance of this part shows predominance of different colours in this part. Parallel to the open fracture light colours are present, whereas in areas remote from the fracture the red or black colours of undisturbed granite are to be seen. As analysis of abraded material results in average element composition, EDX is performed along the blue line and gives the actual element composition of the solids. Results are show in Fig. 10 and Fig. 11.

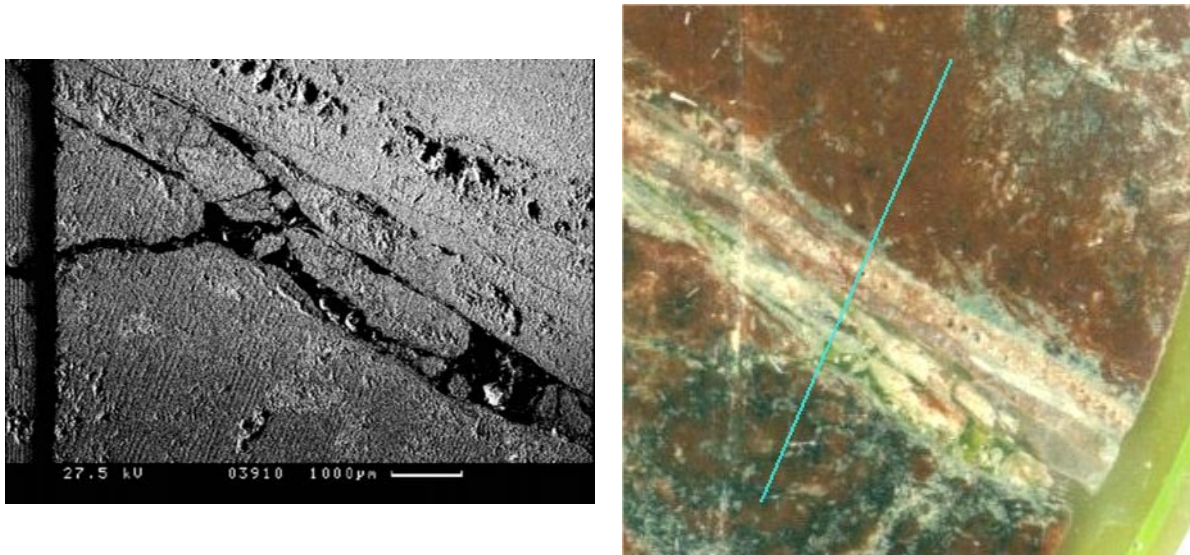


Fig. 9 SEM (left) and optical (right) image of the flow path in the fracture at slice #23 (position C, X = 100 mm).

The black bar in the SEM picture correlates to the white vertical line in the visual picture. The mark is caused by cutting. The blue line in the optical image indicates the SEM/EDX line scan.

EDX is performed at points of about two microns size along the blue line (see Fig. 10). EDX gives the actual relative element composition of the solids. The error of this method depends of the flatness of the surface and is in this case absolute  $\pm 3\%$ .

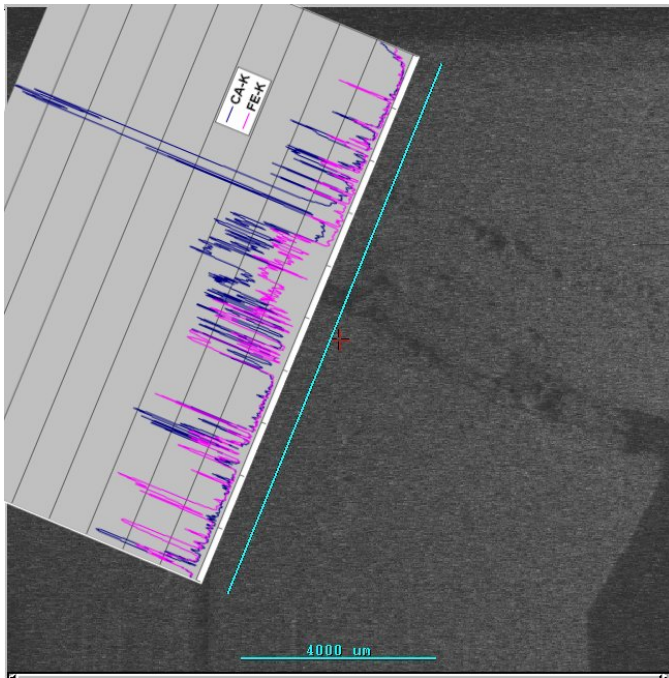


Fig. 10 Ca and Fe distribution along the SEM/EDX line scan in slice 23 (X = 100 mm).

Total length of the line: 10 mm

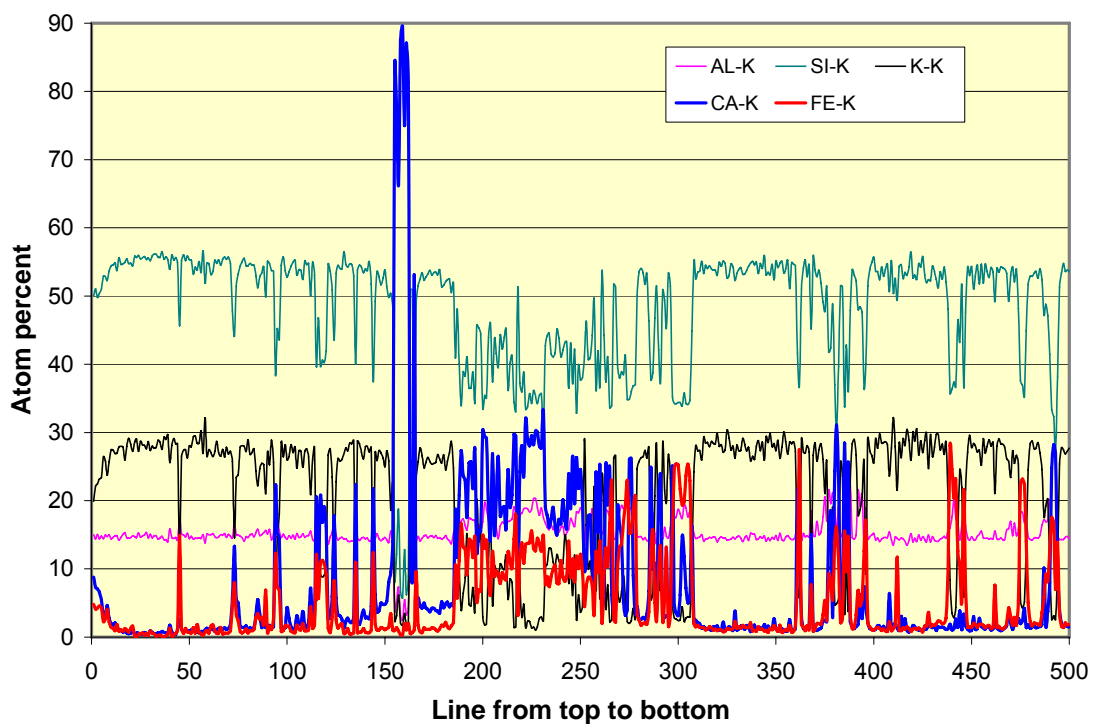


Fig. 11 Main element distributions along the line shown in Fig. 5 and 6 from top to bottom.

In Fig. 10 and Fig. 11 the fracture zone indicated by light colors in Fig. 9) is situated in the range between 150 and 320 steps. At 150 steps from top an almost pure calcium phase occurs having about 90 atom % of Ca and some Si. In this phase, Mg is negligible (not shown in Fig. 11). Light atoms, such as C and O are not detected; a calcium carbonate phase (such as vaterite) may exist there. In the range between 0 and 150 and from 320 to 500 steps, grains of the rock matrix are mapped having about 15 % Al, 28 % K and ~55% Si. Fe and Ca

is located on boundaries, where Si and K concentrations decreased significantly. A correlation between Ca and Mg is not obvious. Average Mg to Ca ratio is calculated to be 0.48, the ratio varies between 0 and 15 indicating different Ca or Mg minerals. An element mapping of a lateral structure is presented in Fig. 12.

In total, the fracture zone is characterized by a high Fe concentration up to 15 atom %. This value is in contrast to other part of the slice, where average values of 2-3 % are found. Within the fracture zone, Si concentration is reduced, which may reflect the presence of epidote  $\text{Ca}_2(\text{Fe}^{(\text{III})},\text{Al})_3(\text{SiO}_4)_3(\text{OH})$  or chlorite which is considered as a clay mineral. The general formula of chlorite is  $\text{X}_{4-6}\text{Y}_4\text{O}_{10}(\text{OH},\text{O})_8$ . The X represents mainly aluminum, iron, or magnesium. The Y represents aluminum and silicon. Epidote is a structurally complex mineral having both single silicate tetrahedrons,  $\text{SiO}_4$ , and double silicate tetrahedrons,  $\text{Si}_2\text{O}_7$ . Two aluminums represent the parallel chains of  $\text{AlO}_6$  and  $\text{AlO}_4(\text{OH})_2$  octahedra of the epidote structure. The silicate groups and extra ions connect the chains together. The color of the fracture zone (see Fig. 9) supports the presence of both phases; epidote is "pistachio" green to yellowish or brownish green. Exact mineralogical characterization of these phases by XRD requires specific sampling techniques which are under development, presently.

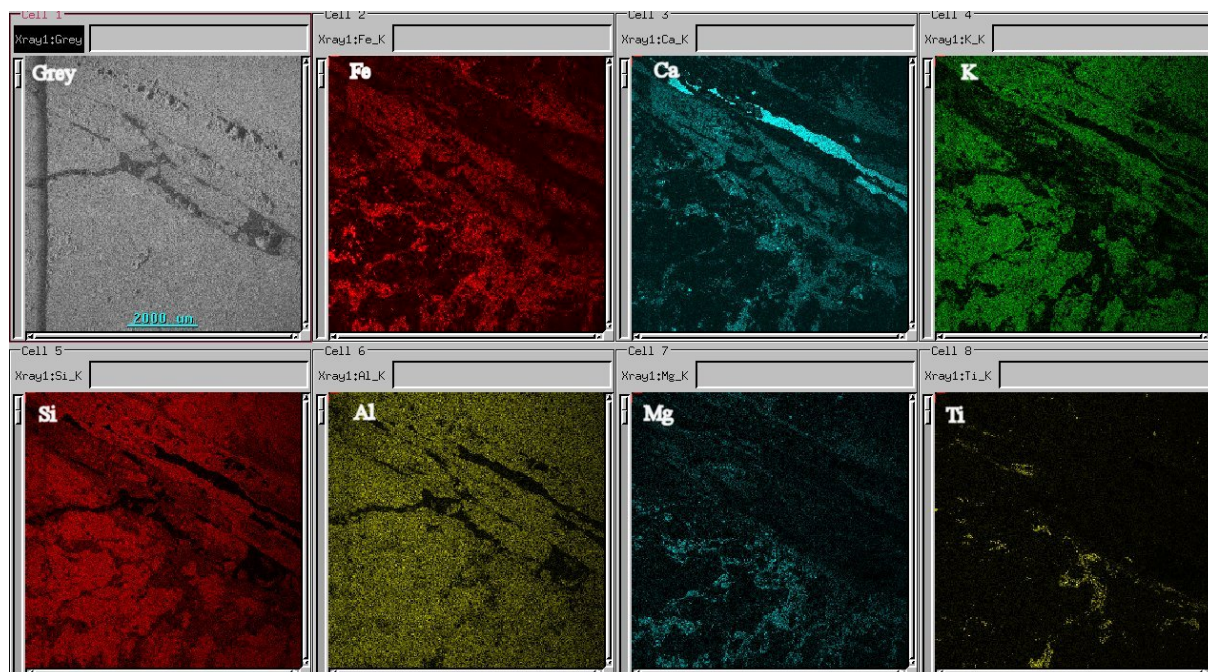


Fig. 12 Lateral element mapping of the fracture zone of slice 23 from core #7.

### 4.3 Uranium retention

In a previous report (Kienzler et al., 2005) batch experiments of U onto altered granite materials are described. These investigations showed that the  $\alpha$ -autoradiogram correlated well with the Fe distribution, and the maxima of retained U coincided with local deposits of Fe oxides. However, to quantify U retention, not only the minerals but also the relevant surfaces and their accessibility are of high importance.

In the previous report (Kienzler et al., 2005), recovery of  $^{233}\text{U}$  of 40 % was reported. This value corresponds well with the retained  $^{233}\text{U}$  which is obtained by integration of the measured  $^{233}\text{U}$  concentrations in the abraded material of core #7 (see Fig. 3). The integration results in a retention of 64 % of the injected U tracer. Of course, both results are subject to errors. Especially in the integration of  $^{233}\text{U}$  concentrations assumptions concerning uniformity of the fracture properties are taken implicitly. Fig. 3 shows a slight increase of  $^{233}\text{U}$  concentration in the range  $80 \text{ mm} \leq X \leq 120 \text{ mm}$ . The pronounced peak at C ( $X \sim 100 \text{ mm}$ ) contributes only about 20 % to the total quantity of retained  $^{233}\text{U}$ .

Considering the maximum  $^{233}\text{U}$  concentration in core #7, the location of this peak can be used to estimate the retention properties of the core. The procedure was described for americium retention in core #5 (Kienzler et al., 2003c) by comparing the velocity of the groundwater with the velocity of the tracer. For core #7 experiment, total eluted volume amounts to 331 ml within 278 days. Assuming a free fracture opening of  $100 \text{ mm}^2$  (see chapter 2, page 2), during the experimental period the ground water moved over a distance of 33100 mm. In the same time, the  $^{233}\text{U}$  retained in the slight shoulder traveled only about 100 mm. Retardation of this fraction of the tracer amounts to  $R_s = 331$ , which is significantly higher than the retention coefficient determined for the mobile U(VI) fraction. From in-situ migration experiment and from batch experiments  $R_s = 3.9$  and  $5.0$ , respectively, were determined. Using this  $R_s$  value, within 278 days, the migration distance would be expected between 6600 mm and 8500 mm. In comparison to the  $^{233}\text{U}$  shoulder at 100 mm in the core #7, the difference is significant. For this reason, one may conclude that a part of the tracer is subject to a different complex retention mechanism. The mechanism may be attributed to

- Specific minerals,
- Different internal surfaces, or
- Slow retention reaction processes such as redox processes.

To get deeper insight into these processes, specific analytical tools are required such as quantification of surfaces under in-situ conditions, preparation and XRD analysis in the scale of the fracture and investigation of the dependence of reaction kinetics on the mineral and their compositions. Special consideration should be given to the Fe(II) to Fe(III) ratio in the minerals. Additionally, modelling of the groundwater flow will show to which extent the splitting-up of the fracture increases the residence time of the tracers at specific locations in the fracture.

$^{233}\text{U(VI)}$  tracer was injected. The same complex retention mechanism should be valid for the natural  $^{238}\text{U}$ , if it exists also in the hexavalent redox state. During the in-situ experiment in total  $\sim 12 \text{ mg } ^{238}\text{U}$  was eluted. Around position C, excess of  $U_{\text{nat}}$  amounts to 360 mg. This means that during the in-situ experiment no significant decrease of the natural uranium accumulation has taken place. An increase of  $U_{\text{nat}}$  at this location by sorption from flowing groundwater can also be excluded due to the low concentrations in the Chemlab 2 drill hole KJ0044F01. Both facts clearly demonstrate that the  $U_{\text{nat}}$  accumulation is of natural origin and not mediated by the experiment or by drilling, etc. Looking to the breakthrough behaviour, it is concluded that both U peaks can be explained by saturation of the rock matrix with oxygen during drilling and storage and matrix diffusion of U(VI) into the open fracture of core #7. The natural uranium profile along the fracture of core #7 do not contradict this hypothesis. However, measured profiles would also support the hypothesis that  $U_{\text{nat}}$  is mobilized mainly from the accumulation around position C in core #7. Batch experiments using U show that the  $\alpha$ -

autoradiogram correlates well with the Fe distribution, and the maxima of retained U coincide with local deposits of Fe oxides (Kienzler et al., 2005).

### 4.4 Technetium retention

Fig. 3 shows the concentration profile of  $^{99}\text{Tc}$  (and  $^{233}\text{U}$  tracers as well as of natural U) determined by dissolution and ICP-MS measurements of the abraded material obtained by slice cutting of core #7. Tc is found close to the detection limit. Only, close to position B and C a concentration up to  $\sim 3.7$  ppb of  $^{99}\text{Tc}$  is measured in the abraded solid material. In position C the Fe concentration is almost twice of the average concentration. However, from analysis of abraded material, a clear correlation between the Tc and the Fe profile cannot be derived. A strong correlation between the Fe and Tc distribution patterns was observed in the batch experiments (Kienzler et al., 2005).

## 5 Conclusions

Combination of information obtained from batch sorption tests, the in-situ migration experiment and the analysis of the internal structure and composition of the core support following conclusions:

- Natural uranium is mobilized from the core in the hexavalent state indicated by the high concentrations in the eluted samples.
- The core was exposed to air before the experiment. The reducing capacity of the system was not sufficient to reduce U(VI) to the tetravalent state.
- During the interruption of the flow, natural and tracer U(VI) diffused from the rock matrix into the fracture increasing the concentration in the water present in the flow path. After restart of the experiment, the elevated concentration decreased according to elution and dispersion
- Natural uranium profile shows maximum concentration at the same position in the rock matrix as the artificial  $^{233}\text{U}$ (VI) tracer.
- $^{99}\text{Tc}$  is retained in the same positions as uranium.
- Maxima of the tracer concentrations and natural uranium correspond to high Fe concentrations. This finding is in agreement with results from batch experiments.

The mechanisms of U and Tc retention are not yet understood completely. Tc is sorbed strongly and the recovery is very small. A major fraction of uranium (40%) migrates and undergoes retention with a low retention coefficient. About 20 % of the initial U tracer is retained at a higher retention coefficient. The higher retention coefficient is correlated to specific mineral phases and mineral surfaces in the flow path.

One may assume, that during the operational phase of a repository, oxygen penetrates into touched fractures inherent in the granite host rock. As a consequence, U(IV) which is present at some 6 ppm in the granite minerals will be oxidized and transferred in a mobile state. The

quantity of oxidized U depends on the number of micro fractures, the distribution of U bearing minerals and certainly on the time during which the repository is open. For this reason in a granite host rock, one can expect that during the operation phase and afterwards a pulse of  $U_{nat}$  migrates according to the groundwater flow. These experiments do not deliver information on estimating the duration of an  $U_{nat}$  pulse. Such a pulse is independent on disposed radioactive wastes and could be studied in mines in comparable geology.

### **Acknowledgment**

The work was performed within the Project Agreement for collaboration on certain experiments related to the disposal of radioactive waste in the Hard Rock Laboratory Äspö (HRL) between the German Bundesministerium für Wirtschaft und Technologie (BMWi) and Svensk Kärnbränslehantering AB (SKB).

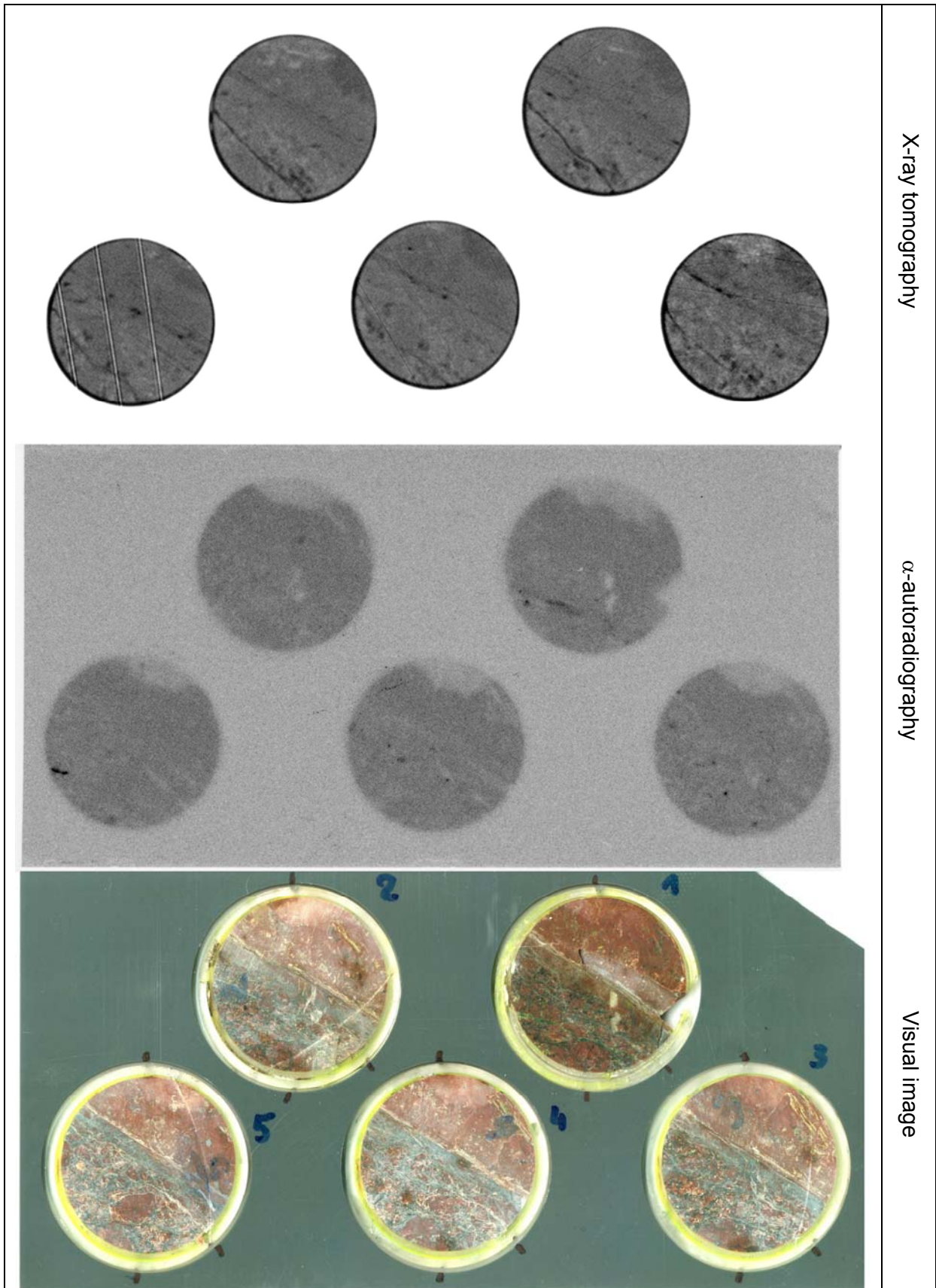
The authors thank the staff of Äspö HRL for preparation of rock and water samples, for the excellent cooperation and the maintenance of our glovebox.

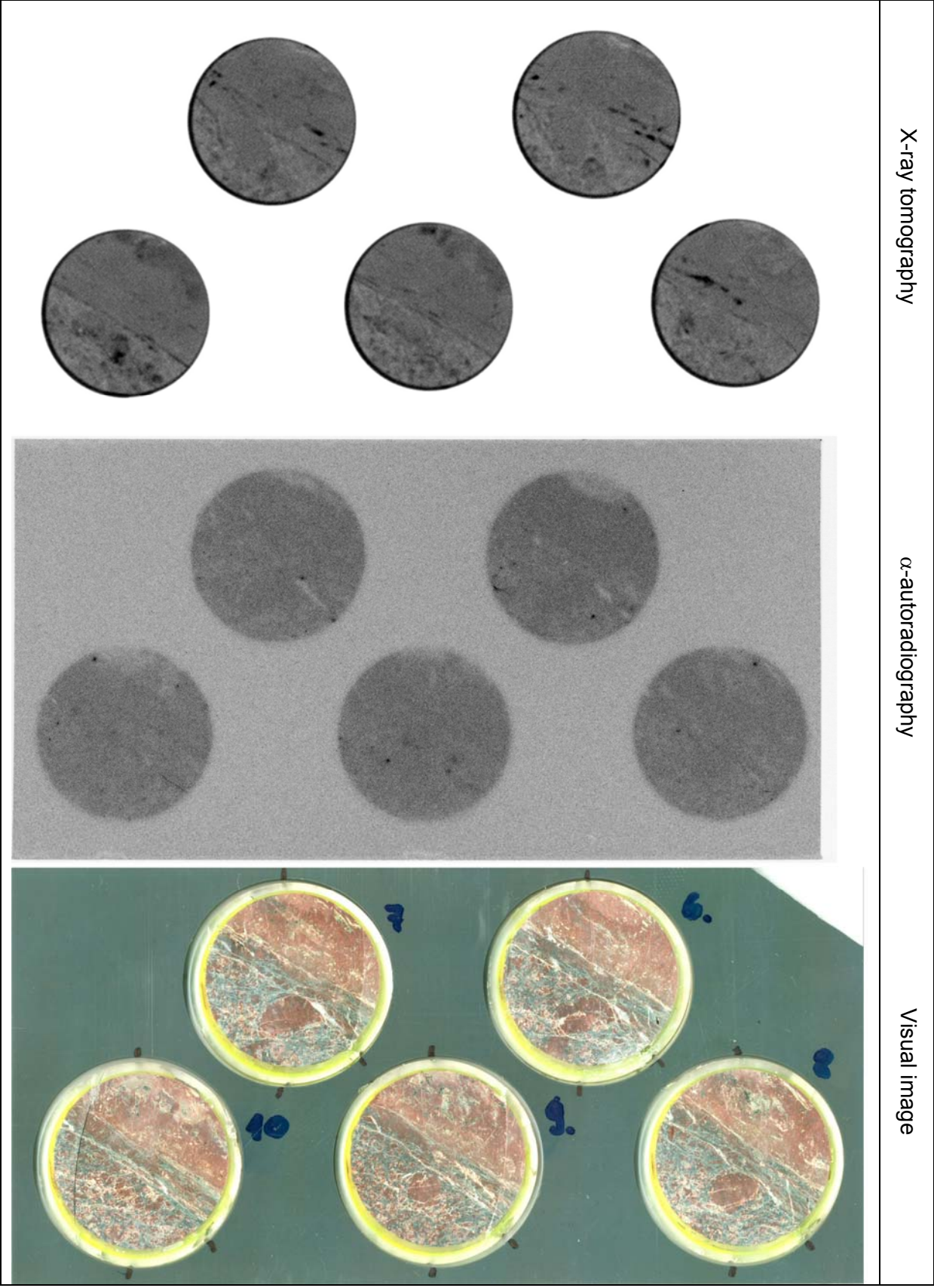
## 6 References

- Bäckblom, G., 1991. The Äspö hard rock laboratory - a step towards the Swedish final repository for high-level radioactive waste. *Tunnelling and Underground Space Technology*, 4: 463-467.
- Jansson, M. and Eriksen, T.E., 1998. CHEMLAB In-Situ Diffusion Experiments Using Radioactive Tracers. *Radiochimica Acta*, 82: 153-166.
- Kienzler, B., Römer, J., Schild, D. and Bernotat, W., 2003a. Sorption of actinides onto granite and altered material from Äspö HRL. In: V.M. Oversby (Editor), *Scientific Basis for Nuclear Waste Management XXVII*. Mat. Res. Soc., Kalmar, June 16-18, 2003.
- Kienzler, B. et al., 2002. Actinide migration in granite fractures: comparison between in-situ and laboratory results, *Scientific Basis for Nuclear Waste Management XXVI*, Symp.II, MRS Fall Meeting, Boston, Mass., December 2-6, 2002.
- Kienzler, B. et al., 2003b. Swedish-German actinide migration experiment at ÄSPÖ HRL. *Journal of Contaminant Hydrology*, 61: 219-233.
- Kienzler, B. et al., 2003c. Actinide migration experiment in the ÄSPÖ HRL in Sweden: results from Core #5 (Part III). FZKA 6925, Forschungszentrum Karlsruhe.
- Kienzler, B. et al., 2005. Actinide Migration Experiment in the ÄSPÖ HRL in Sweden: Results for Uranium and Technetium with Core #7 (Part IV). FZKA 7113, Forschungszentrum Karlsruhe.
- Römer, J. et al., 2002. Actinide migration experiment in the HRL ÄSPÖ, Sweden: results of laboratory and in situ experiments (Part II). FZKA 6770, Forschungszentrum Karlsruhe.
- Vejmelka, P. et al., 2000. Sorption and Migration of Radionuclides in Granite (HRL ÄSPÖ, Sweden). FZKA 6488.
- Vejmelka, P. et al., 2001. Actinide migration experiment in the HRL ÄSPÖ, Sweden: Results of laboratory and in-situ experiments (Part I). FZKA 6652, Forschungszentrum Karlsruhe.



## Appendix A Images of slices of core #7





X-ray tomography

$\alpha$ -autoradiography

Visual image

